Delaying the onset of macrogelation for the synthesis of branched and star-like polymers *via* conventional free-radical polymerisation: Binary solvent effects and incorporation of surfmers

Jing Fung Tan, Anton Blencowe, Greg G. Qiao*

Polymer Science Group, Department of Chemical and Biomolecular Engineering, The University of Melbourne, Parkville, Victoria 3010, Australia

ARTICLE INFO

ABSTRACT

It is known that the preferential solvation and conformation of a polymer in a solvent mixture are functions of the polymer's molecular weight and the solvent qualities. This paper demonstrates that these relationships can be exploited to delay the onset of macrogelation for branched poly(methyl methacrylate/ethylene glycol dimethacrylate) (p(MMA/EGDMA)) polymers and star-like poly(methyl acrylate/ethylene glycol dimethacrylate) (p(MA/EGDMA)) polymers synthesised *via* conventional free-radical polymerisation (CFRP) in a binary solvent mixture (consisting of a good solvent and a precipitant for the polymer). The gelation limits of the MMA/EGDMA and MA/EGDMA polymerisations in a methyl ethyl ketone (MEK)/heptane binary solvent mixture can be extended to regions of higher monomer concentration with increases in polymer yield between 13 and 50 ± 5 w/w% for the p(MMA/EGDMA) system and between 8 and 19 ± 6 w/w% for the p(MA/EGDMA) system across the gelation boundary. Thus, a facile method of increasing the concentration of batch reaction mixtures by the simple addition of small amounts of precipitant into the reaction solutions is presented. Furthermore, the gelation limits of both polymerisation systems in the binary solvent mixtures were further extended with increases in polymer yield between 11 and 17 ± 4%w/w for the p(MMA/ODA/EGDMA) system and between 8 and 20 ± 5%w/w for the p(MA/VS/EGDMA) system by the respective incorporation of octadecyl acrylate (ODA) and vinyl stearate (VS) surfmers into the polymers, demonstrating the application of steric hindance to shield the propagating polymers from excessive cross-linking reactions.

© 2008 Elsevier Ltd. All rights reserved.

1. Introduction

Core cross-linked star (CCS) polymers are well-defined, three-dimensional macromolecules consisting of a central cross-linked core with radiating linear arms [1,2]. These polymers are commonly synthesised *via* living radical polymerisation methods such as nitroxide-mediated radical polymerisation [3], atom transfer radical polymerisation [4,5] or reverse addition–fragmentation chain transfer polymerisation [6]. CCS polymers exhibit unique rheological properties compared to their linear counterparts, such as low viscosity at high M_w, which make them ideal for applications such as binders in paint, rheological modifiers, drug delivery and membrane formation [5,7,8]. However, the environmental and economic costs associated with producing these well-defined polymers *via* living radical polymerisation methods make them only suitable for high value commercial applications. To overcome

these problems in the synthesis of high volume products, we have previously developed a one-pot CFRP process to produce polymers exhibiting similar properties to CCS polymers (termed 'star-like polymers') by controlling the reactivity difference (*r*) between the cross-linker and mono-vinyl monomers used (Schemes 1 and 2) [7].

However, it was realised that these star-like polymers (SLPs) could not be synthesised in highly concentrated solutions as a result of a threshold monomeric concentration. This prevented large amounts of monomers from being fed into the system as macrogelation would occur if the threshold concentration was exceeded, rendering the product unusable.

Polymerisable surfactants (surfmers) are essentially molecules with a long-chained alkyl 'tail' and a polymerisable 'head', with both these components having very different affinities to the solvent used in the reaction. They have been extensively used in emulsion and non-aqueous dispersion polymerisation to stabilise polymer microparticles [9–12]. Derivatives of these surfmers, known as 'macromolecular stabilisers' have also been used in non-aqueous dispersion polymerisation [13]. The evolution from the use of surfmers in aqueous to non-aqueous media and from the synthesis of insoluble to soluble microparticles indicates the
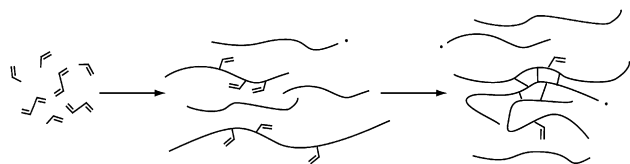
Scheme 1. Mechanism of branched p(MMA/EGDMA) polymer formation when $r_{\text{cross-linker}} > r_{\text{mono-vinyl monomer}}$.
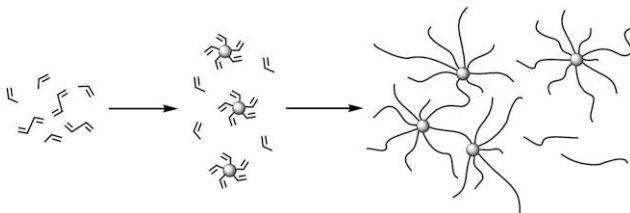
Scheme 2. Mechanism of star-like p(MA/EGDMA) polymer formation when $r_{\text{cross-linker}} \gg r_{\text{mono-vinyl monomer}}$.

potential in this field for realising a method for stabilising soluble SLPs produced by homogeneous solution polymerisation.

The most common method of synthesising polymeric products with an increased tendency to gel has been to carry out the polymerisation in a dilute reaction mixture, which results in the use of an excessive amount of solvent. Recently, Wang et al. reported the successful synthesis of high yielding hyperbranched p(divinyl benzene) (p(DVB)) and p(EGDMA) polymers *via* deactivation enhanced ATRP without resulting in macrogelation of the reaction mixture [14]. Developing a CFRP technique to delay the onset of macrogelation has the added advantage of avoiding the use of environmentally hazardous metal catalysts during the process. Herein, we demonstrate the ability to synthesise high yielding branched and star-like polymers *via* CFRP by increasing the concentration of monomers that can be employed in each batch process, by increasing the macrogelation limit of the synthetic process through the use of a binary solvent system [15] and the incorporation of surfmers into the polymers. An alternative 'monomer–polymer' partitioning hypothesis to the 'monomer–monomer' partitioning theory suggested by Kwok et al. [16] is used to explain this effect, with the conformational changes of the growing polymer chains in the binary solvent mixture believed to be the principle reason behind the success of this partitioning theory. Kinetic data is presented for the MA/EGDMA polymerisation system to support the postulate that the polymers prepared resemble well-defined CCS polymers produced *via* living radical methods. In addition, surfmers are incorporated into these polymers to demonstrate their ability to further prevent macrogelation in concentrated reaction solutions. The proposed mechanisms behind both techniques are supported with relevant experimental results from gel permeation chromatography (GPC), gas chromatography (GC), ^{13}C nuclear magnetic resonance (^{13}C NMR) spectroscopy and dynamic light scattering (DLS). Evidence demonstrating the structural differences between the p(MMA/EGDMA) and p(MA/EGDMA) polymers are also presented, supporting the hypothesis that p(MMA/EGDMA) polymers have a more branch-like structure, whereas the p(MA/EGDMA) polymers are more star-like.

2. Experimental section

2.1. Materials

Methyl methacrylate (MMA, 99%), methyl acrylate (MA, 99%), ethylene glycol dimethacrylate (EGDMA, 98%) were passed over a plug of inhibitor remover and basic alumina (Scharlau) twice to remove any inhibitors present. Octadecyl acrylate (ODA, 97%) and vinyl stearate (VS, 99+%) were used as purchased. All monomers were stored below 4 °C prior to use. 2,2′-Azobis(2-methyl-propionitrile) (AIBN, 98%) (Acros Organics), methyl ethyl ketone (MEK, AR grade) (Chem-Supply), heptane (AR grade) (Ajax Finechem), methanol (GR grade) (Merck) and tetrahydrofuran (THF, HPLC grade) (Merck) were used as received. All reagents were purchased from Sigma–Aldrich unless otherwise specified.

2.2. Characterisation

2.2.1. Determination of monomer conversion by GC

GC analysis was performed on a Shimadzu GC-17A gas chromatograph equipped with a DB-5 capillary column (Phenomenex, solid phase 5% phenylsiloxane and 95% dimethylpolysiloxane; 30 m × 0.25 mm × 0.25 μm) and coupled to a GC–MS-QP5000 electron ionisation mass spectrometer. Aliquots (0.5 mL) of each reaction mixture were precipitated into methanol (1.5 mL) and the supernatant was extracted and passed through a 0.45 μm filter. A total of 5 μL of this filtered sample were then injected into the GC–MS for analysis. Standard curves of known monomer concentrations were generated and used to determine the concentration of residual monomers after each reaction.

2.2.2. Characterisation of synthesised polymers by GPC

Characterisation was carried out on a Shimadzu size-exclusion chromatogram equipped with a Wyatt DAWN EOS MALLS detector (690 nm, 30 mW) and Wyatt OPTILAB DSP interferometric refractometer (690 nm) using Phenomenex Phenogel columns (500, 10^4 and 10^6 Å porosity; 5 μm bead size) operating at 30 °C. THF was used as the eluent at a flowrate of 1 mL/min. Astra software (Wyatt Technology Corp.) was used to determine the molecular weight characteristics using known dn/dc values ($dn/dc_{\text{MMA}} = 0.086$ and $dn/dc_{\text{MA}} = 0.092$) [17] or the injected polymer mass values based on the assumption of 100% mass recovery when the dn/dc values were unknown. Aliquots (1 mL) of each reaction mixture were diluted with an appropriate amount of THF and shaken vigorously to quench the reaction by the introduction of atmospheric oxygen. The samples were then passed through a 0.45 μm filter and injected into the GPC for analysis.

2.2.3. Polymer characterisation by ^{13}C NMR

Characterisation was carried out on a Varian Unity Plus 400 MHz spectrometer. The polymer was isolated through precipitation of the reaction mixture into chilled methanol and dried under vacuum (10 Pa) to yield a white powder. A total of 50 mg of the polymer were then dissolved in 1 mL of deuterated chloroform containing tetramethylsilane (1%v/v) before analysis.

2.2.4. Polymer characterisation by DLS

Dynamic light scattering (DLS) measurements were performed on a Malvern high performance particle sizer (HPPS) with a He–Ne laser (633 nm) at an angle of 173° and a temperature of 25 °C. The polymer was isolated through precipitation of the reaction mixture into chilled methanol and dried under vacuum (10 Pa) to yield a white powder. A total of 10 mg of the polymer were then dissolved in 1 mL of THF. The samples were then passed through a 0.45 μm filter before analysis.

2.3. Synthetic methods

2.3.1. Synthesis of branched MMA/EGDMA and star-like MA/EGDMA polymers

Monomeric compositions of the various mixtures used to determine the polymer domains for the different systems were

based on the definitions of %*M* and %*C* as defined in Equations (1) and (2),

$$\%M = \frac{m_{\text{monomers}}}{m_{\text{mixture}}} \times 100 \qquad (1)$$

$$\%C = \frac{m_{\text{cross-linkers}}}{m_{\text{monomers}}} \times 100 \qquad (2)$$

where *m* denotes the mass of the respective species and m_{mixture} denotes the total mass of the reaction mixture (*i.e.* monomers and solvent). Calculated amounts of the monomers were added into a schlenk tube together with AIBN at a 100:1 molar ratio. The reaction mixture was then mixed and subjected to three freeze-pump-thaw cycles on a vacuum line (10 Pa) to remove any oxygen present in solution. This was followed by back-filling of the tube with argon to restore atmospheric pressure and maintain an inert environment. The schlenk tubes were then immersed into an oil bath that was maintained at 70 °C for 20 h.

For a p(MMA/EGDMA) formulation of 5%*C* and 16%*M* in a binary solvent composition of MEK:heptane (80:20%w/w), MMA (1.07 mL, 9.99 mmol), EGDMA (0.05 mL, 0.27 mmol) and AIBN (16.8 mg, 0.10 mmol) were dissolved in a binary solvent mixture of MEK (5.49 mL) and heptane (1.62 mL). After the required reaction time, the reaction mixture was quenched by introducing atmospheric oxygen and subjected to vigorous shaking. The reaction mixture was then precipitated into chilled methanol to afford a white precipitate. This precipitate was filtered and subsequently dried *in vacuo* (10 Pa) to yield a powdery white solid, 0.74 g (74% yield). GPC: $M_{\text{w}} = 3820$ kDa, PDI = 2.5.

2.3.2. Synthesis of branched MMA/ODA/EGDMA and star-like MA/ODA/EGDMA polymers

With the exception that 10%w/w of the mono-vinyl monomers (MMA or MA) in the above formulation were substituted with the surfmer, ODA, the procedure was conducted in an identical fashion.

2.3.3. Kinetic studies

For the p(MMA/EGDMA) system, a formulation of 3%*C* and 14%*M* was used. MMA (10.7 mL, 99.9 mmol), EGDMA (0.29 mL, 1.56 mmol) and AIBN (170 mg, 1.01 mmol) were dissolved in MEK (78.7 mL) or a binary solvent mixture with a composition of MEK:heptane of 55.1:27.8 mL. The reaction solutions were added to three-necked round-bottomed flasks complete with magnetic stirrer bars, condensers and argon inlets. Septums were placed on all openings and disposable needles were inserted into the septum at the end of the condensers to act as argon outlets. The systems were degassed by bubbling argon through the mixtures for 1 h, after which, the flasks were lowered into preheated oil baths set at 70 °C. A gas-tight syringe was then used to periodically extract samples for analysis.

For the p(MMA) system, a formulation of 0%*C* and 24%*M* was used. MMA (21.4 mL, 200 mmol) and AIBN (328 mg, 2.00 mmol) were dissolved in MEK (78.7 mL) or a binary solvent mixture with a composition of MEK:heptane of 55.1:27.8 mL, depending on the experiment. The rest of the experimental procedure was conducted in an identical fashion to the p(MMA/EGDMA) system.

For the p(MA/EGDMA) system, a formulation of 5%*C* and 18%*M* was used. MA (20.9 mL, 232 mmol), EGDMA (1.00 mL, 5.31 mmol) and AIBN (390 mg, 2.38 mmol) were dissolved in MEK (119 mL) or a binary solvent mixture with a composition of MEK:heptane of 83.4:42.1 mL, depending on the experiment. The rest of the experimental procedure was conducted in an identical fashion to the p(MMA/EGDMA) system.

For the p(MA) system, a formulation of 0%*C* and 27%*M* was used. MA (24.1 mL, 267 mmol) and AIBN (439 mg, 2.67 mmol) were

dissolved in MEK (77.2 mL) or a binary solvent mixture with a composition of MEK:heptane of 54.1:27.3 mL, depending on the experiment. The rest of the experimental procedure was conducted in an identical fashion to the p(MMA/EGDMA) system.

3. Results and discussion

### 3.1. 'Monomer–polymer' partitioning hypothesis

Kwok et al. reported that the formation of gel particles during the synthesis of p(MMA/EGDMA) in a binary solvent could be delayed by the selection of a cross-linker that was soluble in the precipitant for the polymer, which was attributed to 'monomer–monomer' partitioning in the system [16]. However, it seems unlikely that partitioning of the monomers in the initial pre-reaction mixture is the primary cause for the delayed formation of gel particles as conversion-phase diagrams have shown that polymerisation-induced phase separation (PIPS) in a binary solvent system is a function of both monomer conversion and solvent composition [16,18]. Given the solubility of both monomers and the insolubility of the polymeric analogues in the precipitant component of the solvent mixture, it is evident that partitioning would be more pronounced in mixtures comprising of large M_{w} polymers as opposed to monomeric species. Therefore, the delayed formation of gel particles in binary solvent systems is better described by a 'monomer–polymer' partitioning theory. It has been demonstrated that polymerisation in poor solvents leads to the polymers adopting a more coiled conformation as a result of the poor solvating environment in their vicinity [19,20]. There have also been numerous studies on the preferential solvation of polymers in binary solvent systems, which have shown that the polymer chains preferentially adsorb solvent molecules of one component of the solvent mixture [21] and that the greatest dependence is exhibited in solvent mixtures consisting of a good solvent and a precipitant of the polymer [22]. Therefore, it is expected that the propagating polymers in a binary solvent mixture would attempt to orientate themselves to be preferentially solvated by the good solvent component of the mixture as the reaction progresses.

To further elucidate the mechanism responsible for the delayed formation of gel particles in binary solvent systems, the CFRP of MMA/EGDMA and MA/EGDMA monomer systems were conducted in MEK/heptane mixtures. It is proposed that in a pre-reaction mixture consisting of monomers (mono-vinyl monomers and di-vinyl cross-linkers) and initiator in a binary solvent system, the monomers are solvated by both solvent components as the solubility of monomers is dependent on both their solubility parameters and molecular weight. Thus, low molecular weight species such as monomers are soluble in the precipitant component (heptane) of the solvent system (*i.e.* MMA or MA in heptane) even though the solubility parameters of both these monomers are considerably different from the precipitant component (Table 1).

As the polymerisation progresses, the increasing M_{w} of the growing polymer chains would begin to exert a greater influence on

Table 1
Solubility parameters of solvents and reactants used [13,17,25].

Reagent	Solubility parameter δ (MPa$^{0.5}$)
MMA	18.0
p(MMA)	18.3
MA	18.2
p(MA)	18.2
EGDMA	18.6
p(ODA)	16.3
MEK	19.0
Heptane	15.1

(Non-solvent molecule: ●, solvent molecule: ○, monomer: ⌒)
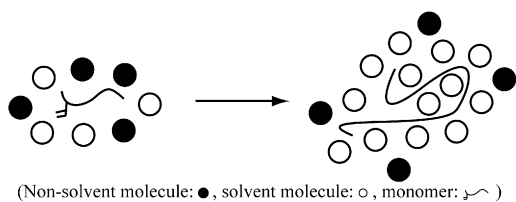
Scheme 3. Preferential solvation in a binary solvent mixture.

their solubility. As a result, the propagating polymers orientate themselves away from the precipitant component of the mixture to minimise their Gibbs free energy [18] while the monomers exist in equilibrium between both solvents (Scheme 3). For example, Archer et al. have modelled the behaviour of polymers in a binary solvent mixture by using large Gaussian core particles immersed in a binary mixture of smaller Gaussian particles close to fluid–fluid phase separation, and have shown that attractive long-range solvent mediated potentials exist between the large Gaussian core particles [23]. These potentials would result in most of the polymers concentrating in a good solvent environment with a solvent-cage of good solvent molecules surrounding the growing polymer chains, while the precipitant environment would contain a low polymer concentration as a result of the polymers transferring out of that environment [24].

As the polymerisation progresses, the increased polymer concentration in the good solvent environment leads to a relative reduction in the amount of monomers in the polymers vicinity as the monomers are distributed in both the good and precipitant solvent environments. This confines the propagation of these polymers to environments which have a lower monomeric content as compared to an overall 'unpartitioned' mixture. The sparing solubility of the initiator in the precipitant also contributes to the bulk of the polymerisation occurring in the good solvent environment. Therefore, in a system where the good solvent is the major component, appropriate amounts of precipitant added to the system would enable a greater concentration of monomers to be employed without resulting in gelation before the onset of PIPS.

3.2. Determination of the optimal solvent composition

The branched p(MMA/EGDMA) and star-like p(MA/EGDMA) polymers were synthesised *via* CFRP following the methodology of Ho et al. [7] Initially, a series of experiments involving the copolymerisation of MA and EGDMA were carried out with varying solvent compositions of MEK/heptane at a formulation of 1%*C* and 34%*M*, to determine the solvent composition at which PIPS would be induced. This formulation, which is beyond the gelation limit in a mono-solvent system (*i.e.* macrogelation occurred when reactions using this formulation were carried out in a mono-solvent system) was chosen to demonstrate the delayed macrogelation in the binary solvent mixture. Similar experiments were carried out for the p(MMA/EGDMA) system at a formulation of 5%*C* and 16%*M*. It was found that a solvent composition between 20 and 30%w/w heptane effectively delayed macrogelation (Table 2) in both systems.

The results observed for the p(MA/EGDMA) system at 10, 20 and 30%w/w heptane are also represented in Fig. 1. Whereas polymerisations conducted using 10 and 30%w/w heptane resulted in the formation of gels, the reaction conducted in 20%w/w heptane yielded a soluble polymer which remained in solution. These observations can be explained by elaborating on the role played by the precipitant during the polymerisation. When low amounts of heptane were added to the system (Table 2, Expt. 2), the onset of macrogelation was not delayed as the monomeric concentration in the vicinity of the propagating polymers in the MEK environment

Table 2
Copolymerisation of MA/EGDMA and MMA/EGDMA with varying heptane concentrations at 70 °C for 20 h, using AIBN as the initiator.

Expt	Mono-vinyl monomer	Formulation		Solvent composition %w/w heptane	Observation
		%*C*	%*M*		
1	MA	1	34	0	Clear gel
2	MA	1	34	10	Clear gel
3	**MA**	**1**	**34**	**20**	**Clear solution**
4	MA	1	34	30	Opaque gel
5	MMA	5	16	0	Clear gel
6	MMA	5	16	10	Clear gel
7	**MMA**	**5**	**16**	**20**	**Clear solution**
8	MMA	5	16	30	Opalescent solution[a]

[a] The opalescent solution became homogeneous upon dilution with THF.

was not lowered sufficiently. In comparison, the desired result was observed when an optimum amount of heptane (Table 2, Expt. 3) prevented the onset of gelation without the occurrence of PIPS. Further increases in the heptane concentration (Table 2, Expt. 4) would result in PIPS being induced as the good solvent environment would be insufficient to solvate all the propagating polymer chains. As a result, the increased unfavourable environment would cause the polymers to aggregate together, forcing the vinyl groups together and increasing intermolecular reaction, thus resulting in a phase-separated macrogel.

3.3. p(MMA/EGDMA) system

To illustrate the effectiveness of delaying the onset of macrogelation by exploiting the preferential solvation behaviour of the polymers, a series of reactions were conducted at different %*C* and %*M* formulations. Experiments were carried out with two solvent compositions of MEK:heptane (80:20 and 70:30%w/w) to determine, if any, the effect of the binary solvent composition on delaying the onset of gelation. The results for the p(MMA/EGDMA) system are presented in the form of a polymer domain diagram (Fig. 2). Large and small symbols denote the formation of insoluble polymers and soluble polymers, respectively.

The domain diagram indicates that the gelation limit for the polymer system was extended into regions of higher monomeric content when a binary solvent mixture was employed, with increases of 2–14%*M*, equating to an increase in polymer yield of 13–50 ± 5 w/w% across the boundary [26]. Fig. 2 also reveals that the 80:20 and 70:30%w/w MEK:heptane gelation boundaries for the p(MMA/EGDMA) system are similar.
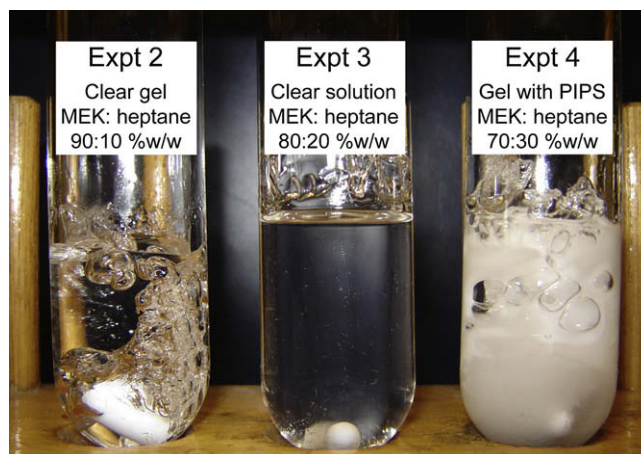

Fig. 1. Photograph of the effect of precipitant addition to p(MA/EGDMA) SLP systems synthesised by CFRP in MEK at 1%*C* and 34%*M*. Experiments were conducted at 70 °C for 20 h, using AIBN as the initiator.
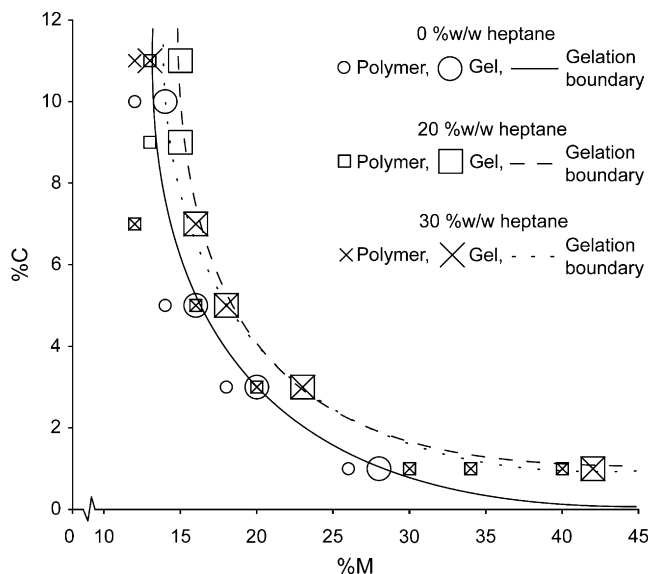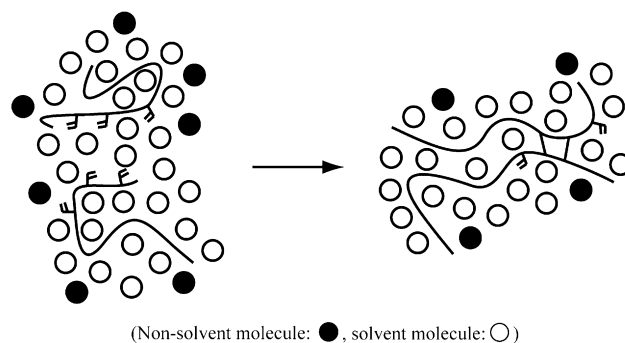
Fig. 2. Domain diagram for p(MMA/EGDMA) SLPs synthesised by CRFP in pure MEK, MEK:heptane 80:20 and 70:30%w/w at 70 °C for 20 h, using AIBN as the initiator.

(Non-solvent molecule: ●, solvent molecule: ○)

Scheme 4. Postulated p(MMA/EGDMA) polymer behaviour in a binary solvent mixture.

GPC–MALLS analysis of the polymers (Table 3) produced in the binary solvent mixtures exhibited M_w trends which were dependent on both solvent composition and cross-linker concentration. The M_w of the polymers formed was found to increase with increasing heptane concentration at any particular formulation.

The observed increase in M_w with increasing heptane concentration for the p(MMA/EGDMA) system results from an increase in the concentration of polymer chains in the MEK environment, thus increasing the probability of intermolecular cross-linking and leading to the formation of highly branched macromolecules (Scheme 4). Further evidence of the branched structure of the polymers is provided by the gradient (α) of the conformational plot obtained from the GPC–MALLS data. Given that the theoretical value of α for spheres, random coils in theta solvents and rigid rods are 0.33, 0.60 and 1.0 [27], respectively, the values for the synthesised polymers indicate that branching is present within the polymeric structure (Table 3).

To further evaluate the mechanisms responsible for the M_w trend observed for the p(MMA/EGDMA) system in the binary solvent mixtures, kinetic studies were conducted to monitor the consumption of monomers and evolution of M_w over time. The p(MMA/EGDMA) system was investigated at a formulation of 3%C and 14%M in a binary solvent mixture of 70:30%w/w MEK:heptane and compared to the same reaction conducted in pure MEK. Similar experiments were also carried out for the homopolymerisation of MMA in the absence of EGDMA at a formulation of 0%C and 24%M to determine the effect of the cross-linker on the polymerisation mechanism of branched polymer formation. The monomer

conversion and change in M_w of the MMA/EGDMA and MMA polymerisations with reaction time are presented in Fig. 3.

Fig. 3a and c show that the overall conversions of monomers in both solvent systems are similar, indicating that the extension of the gelation limit was not caused by a decrease in monomer conversion in the binary solvent system as a result of the addition of heptane. However, the conversion rates of MMA and EGDMA in the MEK/heptane mixtures during the polymerisation for both polymerisation systems were consistently lower than the conversion rates in the pure MEK systems. This is in agreement with the hypothesis that the propagating polymer chains residing in the MEK environment in the binary solvent mixture have a lower concentration of monomers in their vicinity, thus the rate of monomer addition to these chains is slower. The sigmoidal shapes of Fig. 3a are due to the solvent viscosity dependence of the overall rate constant for termination as reported in previous studies for MMA polymerisation by Balke and Hamielec [28]. The absence of these shapes in Fig. 3c is due to the rapid formation of high M_w species during the early stages of polymerisation which results in the Norrish–Trommsdorff effect occurring much earlier.

Time-dependent GPC RI traces for the p(MMA) (Fig. 4a and b) and p(MMA/EGDMA) (Fig. 4c and d) systems revealed that the reactions in both solvent systems undergo similar polymerisation mechanisms by virtue of their similar peak shapes, indicating that the addition of heptane does not influence the mechanism. The broadening of Peak 1 at a retention volume of 23 mL (Fig. 4c and d) with time indicated the formation of high M_w branched polymers (1) and linear polymers (2) as illustrated in Scheme 5. This is in contrast to the peak shifts towards high retention volumes observed in Fig. 4a and b, which are due to the formation of low M_w linear polymers, analogous to (2) (Scheme 5). The initial increase in M_w followed by a gradual decrease observed in Fig. 3b is due to the propagating polymers generated during the initial stages of polymerisation depleting the monomers present in solution. As a result, during the latter stages of the polymerisation process, the continuous generation of radicals from the initiators present in solution

Table 3
M_w characterisation of branched p(MMA/EGDMA) polymers in MEK/heptane solvent mixtures at various formulations.

Polymer	Mono-vinyl monomer	Formulation		Solvent composition %w/w heptane	M_w[a] (kDa)	PDI[a]	Yield[b] (%)	α[a]
		%C	%M					
P1a	MMA	3	20	20	1130	10.1	74.0	0.45
P1b	MMA	3	20	30	5600	3.7	70.8	0.54
P1c	MMA	5	16	20	3820	2.5	76.0	0.57
P1d	MMA	5	16	30	5530	4.6	73.7	0.53
P1e	MMA	7	12	20	493	5.7	78.7	0.39
P1f	MMA	7	12	30	814	11.8	74.0	0.48

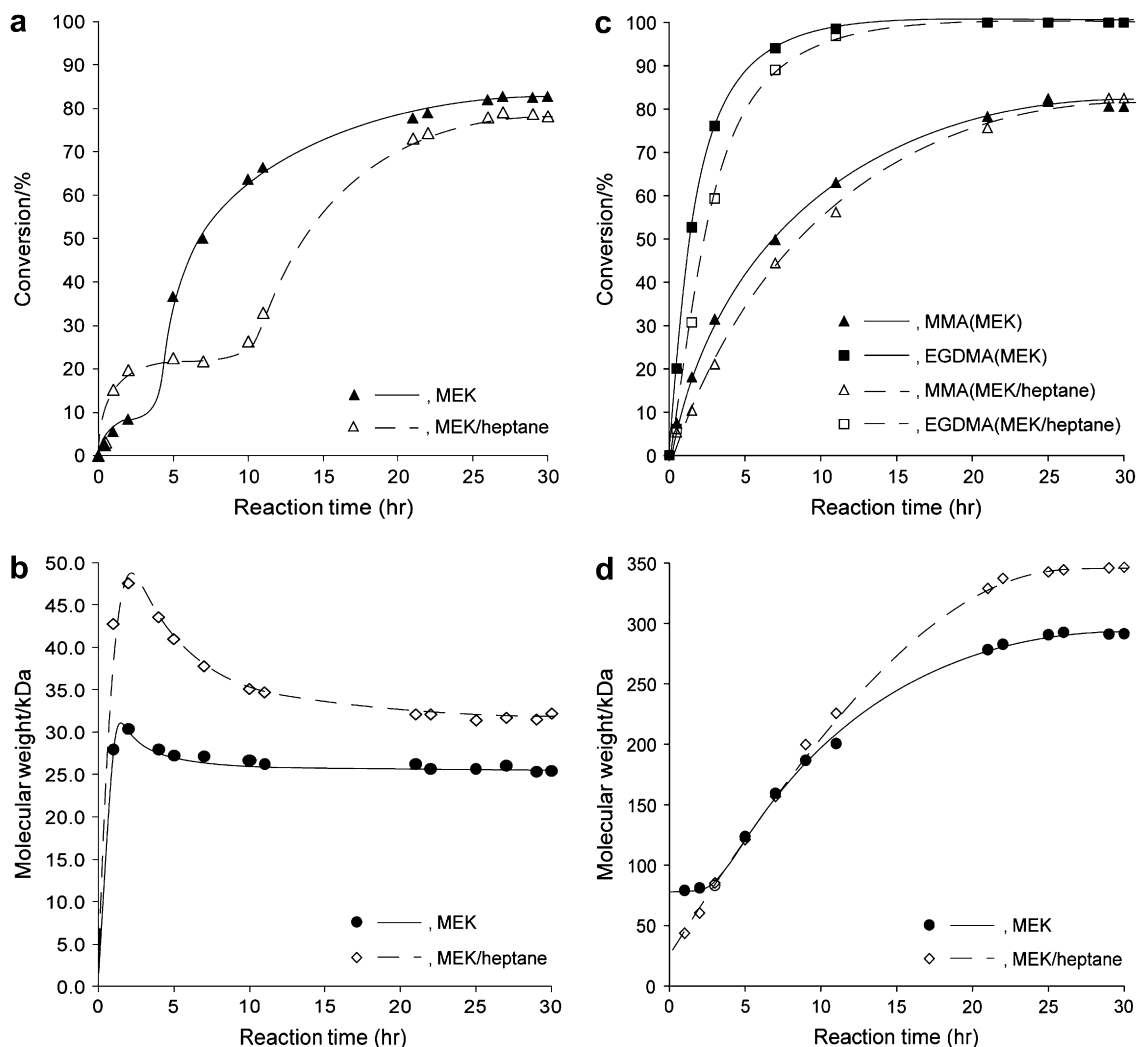[a] Determined by GPC–MALLS.
[b] Determined gravimetrically.

Fig. 3. (a) Conversion of monomers and (b) evolution of M_w with reaction time (30 h) for the homopolymerisation of MMA at a formulation of 0%C and 24%M. MMA conversion after 30 h for the pure MEK and MEK/heptane solvent systems were 83 and 79%, respectively. After 30 h, the polymers produced in pure MEK and MEK/heptane solvent systems possessed M_ws of 26 kDa (PDI = 1.3) and 32 kDa (PDI = 1.3), respectively. (c) Conversion of monomers and (d) evolution of M_w with reaction time (30 h) for the polymerisation of MMA/EGDMA at a formulation of 3%C and 14%M. MMA conversion after 30 h for the pure MEK and MEK/heptane solvent systems were 81 and 83%, respectively. After 30 h, the polymers produced in pure MEK and MEK/heptane solvent systems possessed M_ws of 291 kDa (PDI = 9.8) and 347 kDa (PDI = 9.7), respectively.

results in an increased formation of lower M_w polymers, decreasing the overall M_w of the polymers.

In addition, the GPC RI traces for the MMA/EGDMA polymerisation conducted in MEK/heptane (Fig. 4c) display a more pronounced broadening behaviour. This is a consequence of the concentration effect discussed previously, which brings propagating polymers in a similar solvating environment in close proximity, thus increasing intermolecular cross-linking. This observation is not present for the homopolymerisation of MMA (Fig. 4a) due to the absence of pendent vinyl groups on the propagating polymers, preventing intermolecular cross-linking from occurring. The higher M_w of the p(MMA) homopolymer in the MEK/heptane mixture compared to pure MEK is due to the reduction in the rate of termination events resulting from the coiled conformation adopted by the propagating polymers in a poor solvating environment [19,20].

3.4. p(MA/EGDMA) system

The polymer domain diagram for the p(MA/EGDMA) system is presented in Fig. 5. Large and small symbols denote the formation of insoluble polymers and soluble polymers, respectively. Fig. 5

indicates that the gelation limit for the polymer system was extended into regions of higher monomeric content when a binary solvent mixture was employed, with increases of 2–6%M, which equates to an increase in polymer yield of 8–19 ± 6 w/w% across the gelation boundary [26]. Fig. 5 also reveals that a 80:20%w/w MEK:heptane solvent mixture was more effective in delaying macrogelation at higher %C formulations with a cross-over in efficiency at *ca.* 4%C.

GPC–MALLS analysis of the polymers (Table 4) produced in the binary solvent mixtures exhibited an inverse M_w trend with increasing heptane concentration, in contrast to the increasing M_w trend observed for the p(MMA/EGDMA) polymers (Table 3). It was also revealed that the difference in α values of the p(MA/EGDMA) ($\alpha = 0.25$–0.37) and p(MMA/EGDMA) ($\alpha = 0.39$–0.57) polymers indicate that the p(MA/EGDMA) SLPs have a more spherical structure than the branched p(MMA/EGDMA) polymers. It was also noticed that the α values of the p(MA/EGDMA) SLPs correspond very closely to those of well-defined poly(isoprene/DVB) CCS polymers synthesised using anionic polymerisation ($\alpha_{\text{p(isoprene/DVB) CCS polymers}} = 0.34$), providing further support for the proposed SLP structure [29]. It should be noted that the relationship between the radius of gyration and molecular weight is more complicated than
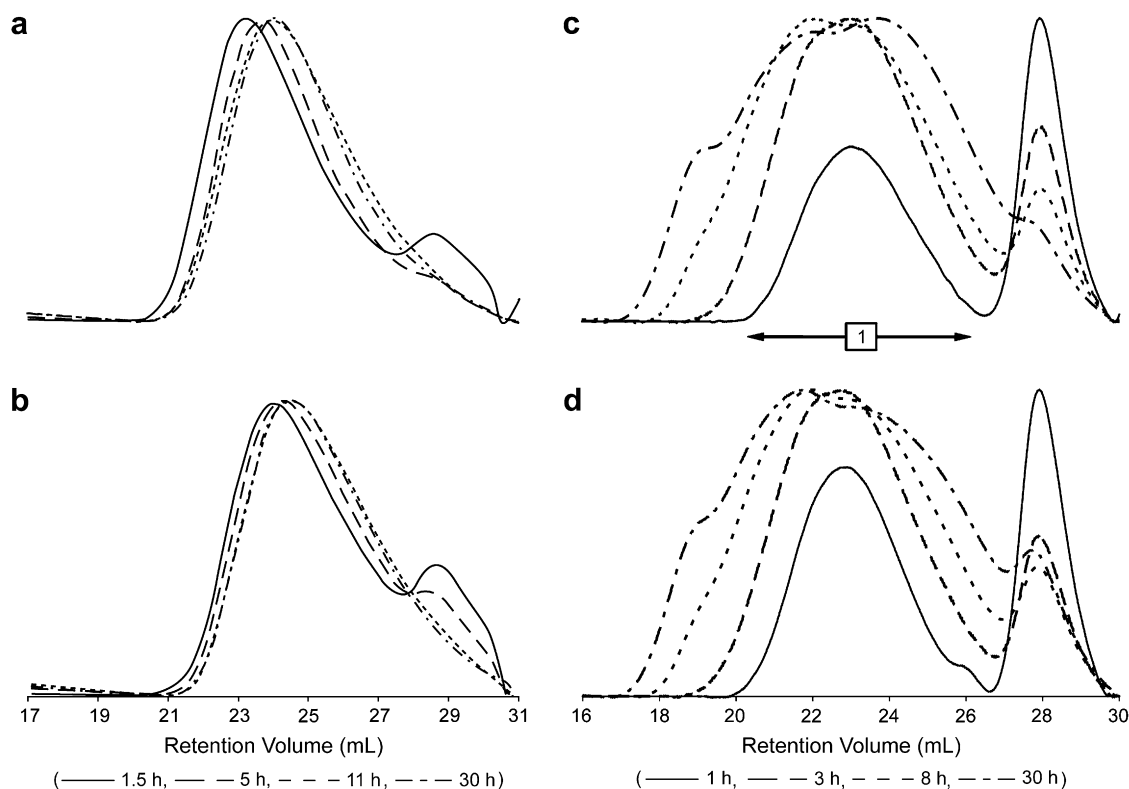
Fig. 4. Time-dependent GPC RI traces for p(MMA) homopolymers prepared at 0%*C* and 24%*M* in (a) 70:30%w/w MEK:heptane and (b) pure MEK and branched p(MMA/EGDMA) polymers prepared at 3%*C* and 14%*M* in (c) 70:30%w/w MEK:heptane and (d) pure MEK.

the α values quoted for spheres, random coils in theta solvents and rigid rods. Given that in this study, the 'star-like' polymers are prepared *via* CFRP and a one-pot approach, they are not precise star polymers which make it very difficult to assign exponents relating to the star's arm length and number [30]. As such, a comparison of p(MA/EGDMA) SLP and well-defined CCS polymer α values is a simplified approach in determining the architecture of p(MA/EGDMA) SLPs.

The p(MA/EGDMA) system was further investigated *via* kinetic studies at a formulation of 5%*C* and 18%*M* in a binary solvent mixture of 70:30%w/w MEK:heptane and as before, compared to the same reaction conducted in pure MEK. Similar experiments were again carried out for homopolymerisation of MA in the absence of EGDMA at a formulation of 0%*C* and 27%*M*. The monomer conversions and change in M_ws of the MA and MA/EGDMA polymerisations with reaction time are presented in Fig. 6.

As with the p(MMA/EGDMA) system, the conversion rates of MA and EGDMA in the MEK/heptane mixture were consistently lower than those in the pure MEK system at a given time, which is

attributed to the reduction in monomeric concentration in the vicinity of the propagating polymers in a binary solvent mixture. However, the M_w trend observed for the p(MA/EGDMA) system was distinctly different to that for the p(MMA/EGDMA) system, with a rapid evolution in M_w initially, followed by a gradual decrease (Fig. 6d). The different M_w profiles for the p(MA/EGDMA) and p(MMA/EGDMA) systems can be explained by analysing the differences in reactivity of the monomers involved in both systems.
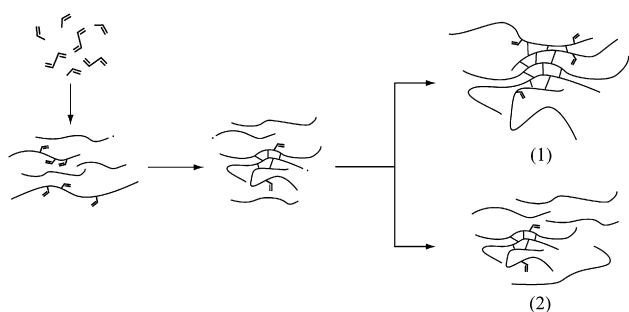
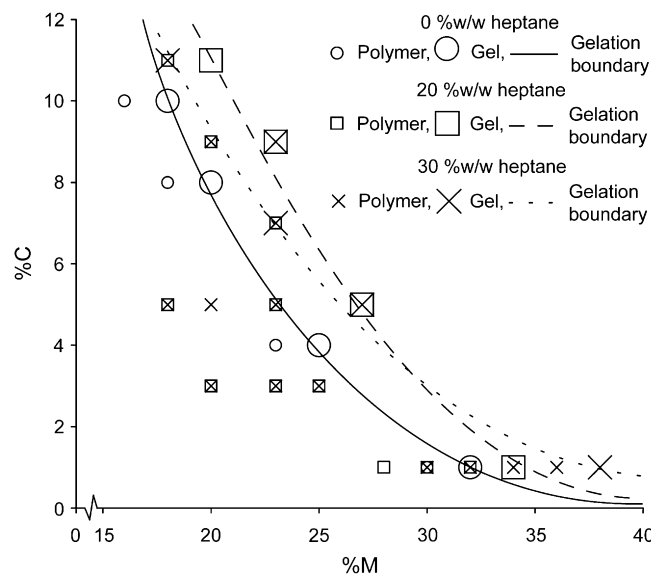**Scheme 5.** Mechanism of p(MMA/EGDMA) polymer formation.

Fig. 5. Domain diagram for star-like p(MA/EGDMA) polymers synthesised by CRFP in pure MEK, MEK:heptane 80:20 and 70:30%w/w at 70 °C for 20 h, using AIBN as the initiator.

Table 4
M_w characterisation of star-like p(MA/EGDMA) polymers in MEK/heptane solvent mixtures at various formulations.

Polymer	Mono-vinyl monomer	Formulation		Solvent composition %w/w heptane	M_w^a (kDa)	PDI[a]	Yield[b] (%)	α^a
		%C	%M					
P2a	MA	3	25	20	668	7.7	52.5	0.37
P2b	MA	3	25	30	109	3.7	50.4	0.25
P2c	MA	5	23	20	1950	4.5	44.4	0.34
P2d	MA	5	23	30	184	9.1	43.9	0.34
P2e	MA	9	20	20	3260	5.6	58.7	0.35
P2f	MA	9	20	30	1320	9.5	52.8	0.34

  [a] Determined by GPC–MALLS.
  [b] Determined gravimetrically.

The methyl group α to the carbonyl group on MMA imparts a greater reactivity to the monomer compared to MA, corresponding to studies on their reactivity ratios [31]. Assuming that the reactivity of EGDMA and MMA is solely dependent on the number of terminal vinyl groups, it can be estimated that the reactivity of EGDMA would be double that of MMA. For the copolymerisation of MMA and MA, the reactivity ratios between $M_1 = $ MMA and $M_2 = $ MA were reported to be $r_1 = 2.15 \pm 0.04$ and $r_2 = 0.40 \pm 0.12$ [17]. Therefore, the reactivity of EGDMA would be around 10 times that of MA. As a result of the increased difference in the reactivity between MA and EGDMA, during the initial stages of the p(MA/EGDMA) polymerisation, EGDMA is consumed more
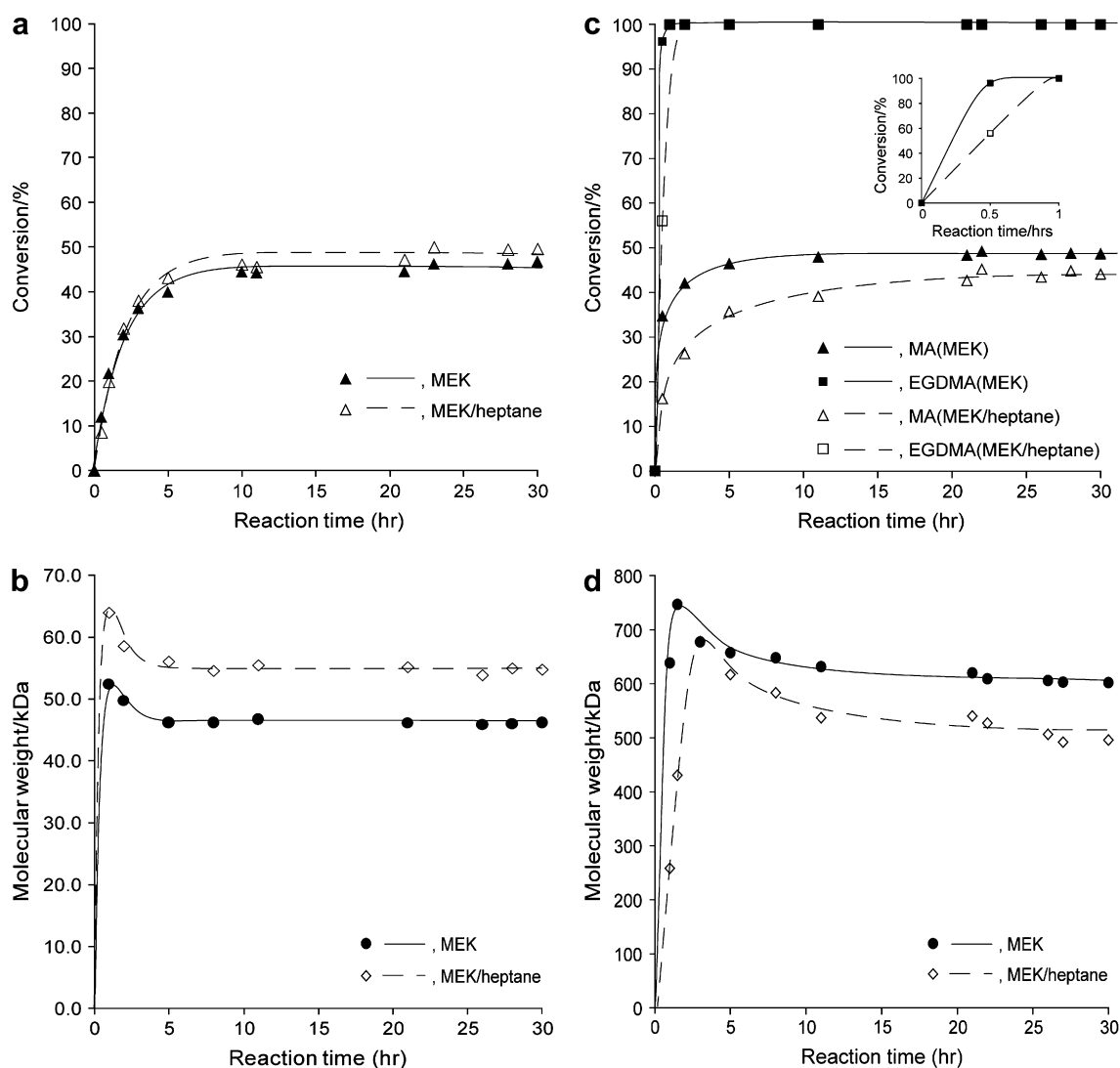

Fig. 6. (a) Conversion of monomers and (b) evolution of M_w with reaction time (30 h) for the homopolymerisation of MA at a formulation of 0%C and 27%M. MA conversion after 30 h for the pure MEK and MEK/heptane solvent systems were 47 and 50%, respectively. After 30 h, the polymers produced in pure MEK and MEK/heptane solvent systems possessed M_ws of 46 kDa (PDI = 1.4) and 55 kDa (PDI = 1.4), respectively. (c) Conversion of monomers and (d) evolution of M_w with reaction time (30 h) for the polymerisation of MA/EGDMA at a formulation of 5%C and 18%M. Inset shows the cross-linker conversion during the first hour. MA conversion after 30 h for the pure MEK and MEK/heptane solvent systems were 49 and 44%, respectively. After 30 h, the SLPs produced in pure MEK and MEK/heptane solvent systems possessed M_ws of 602 kDa (PDI = 7.8) and 496 kDa (PDI = 7.7), respectively.
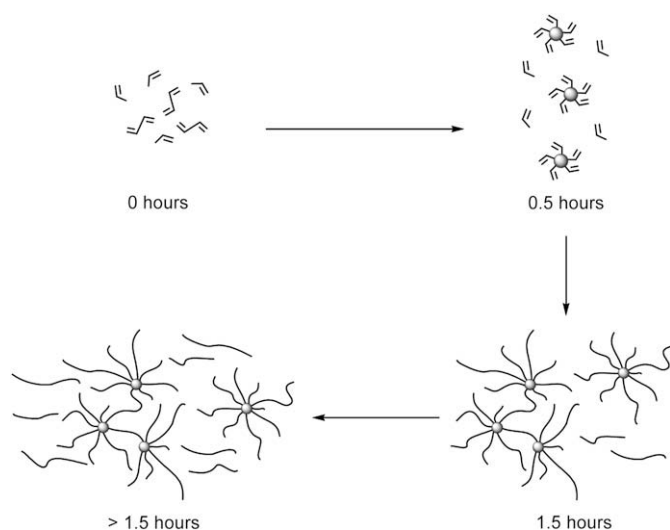
Scheme 6. Mechanism of star-like p(MA/EGDMA) polymer formation.

rapidly relative to MA. Figs. 3c and 6c illustrate this point as the complete consumption of EGDMA in the p(MMA/EGDMA) system is achieved after 10 h, whereas the consumption of EGDMA is completed within 30 min for the p(MA/EGDMA) system. This would result in the formation of dense 'core-like' structures with pendent vinyl groups during the early stages of the MA/EGDMA polymerisation. As the polymerisation progresses, the depletion of EGDMA would result in the increased consumption of MA, which propagates through the unreacted pendent double bonds on these cores, forming the 'linear arms' of the SLPs, thus leading to a rapid increase in M_w (Scheme 6) [7].

Fig. 6d shows that the largest M_w species for each experiment are formed at the 1.5 h mark (783 kDa) for the MEK experiment and 2 h (684 kDa) for the MEK/heptane experiment. This corresponds to the formation of SLPs shortly after the complete conversion of EGDMA at the 30 min mark. Subsequently, the M_ws of the polymers decreased with time. This is attributed to the increased formation of linear p(MA) homopolymers, which would be the dominant chain growth reaction during the latter stages of the polymerisation. The time-dependent GPC RI traces at selected times for the p(MA) and p(MA/EGDMA) systems in pure MEK and the MEK/heptane mixture are presented in Fig. 7.

The high M_w shoulders demarcated by Region 1 in Fig. 7c and d represent the formation of the SLPs during the initial stages of the polymerisation. This shoulder, which formed after the first hour, did not change in retention volume with reaction time, indicating that these sterically hindered SLPs were not susceptible to further polymerisation as a result of the cores being less accessible to attack from propagating homopolymer chains. However, there was a shift in the major peak (Fig. 7c and d, Region 2) into regions of higher retention volumes, indicating the formation of lower M_w species. This is attributed to the formation of linear p(MA) homopolymers as result of the complete consumption of the EGDMA cross-linker during the initial stages of the reaction. The greater reactivity difference between the cross-linker and mono-vinyl monomer also contributes to the formation of the p(MA) homopolymers as it results in a greater probability for compositional drift [32].

This behaviour is in contrast to the p(MMA/EGDMA) polymerisation, where after the initial reaction of the first EGDMA vinyl bond, the reactivity of the second vinyl group would be similar to that of the MMA vinyl group. This would result in a more statistical addition of MMA and EGDMA into the propagating chains producing polymers with more branch-like architectures (Scheme 5). The unreacted pendent double bonds of these p(MMA/EGDMA) polymers are not confined to a core but are distributed throughout the polymer, rendering them more susceptible to grafting and intermolecular cross-linking.

Given the similar peak shapes in both Fig. 7c and d, it can be concluded that the addition of heptane to the p(MA/EGDMA)
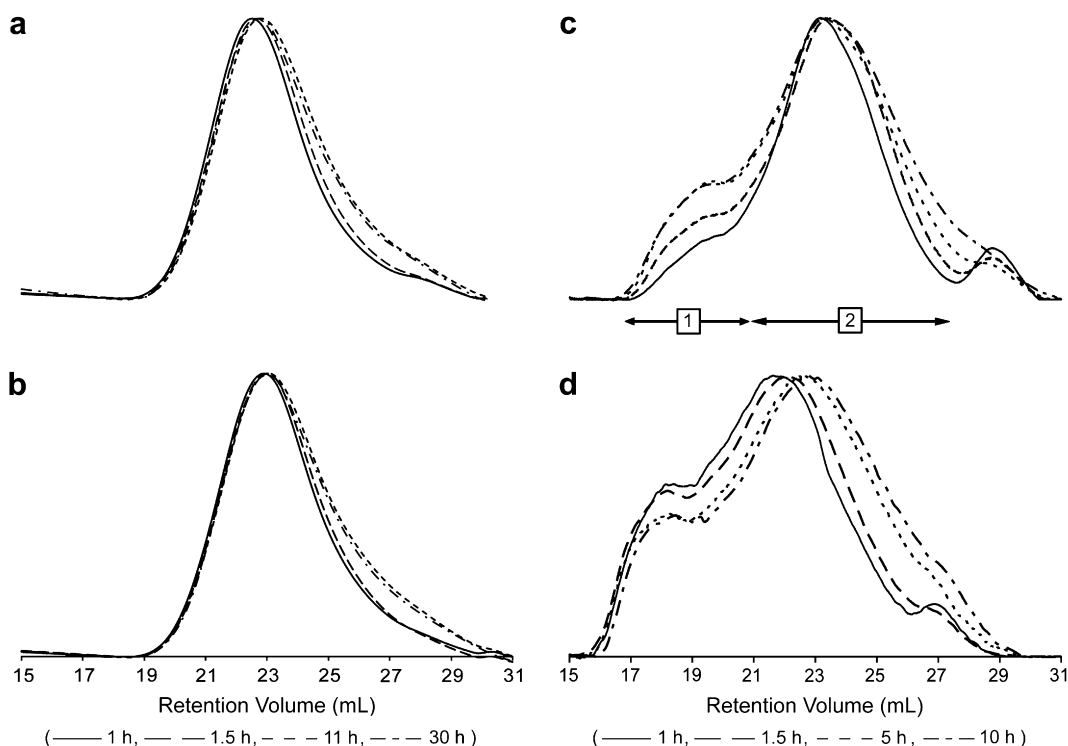

Fig. 7. Time-dependent GPC RI traces for p(MA) homopolymers prepared at 0%C and 27%M in (a) 70:30%w/w MEK:heptane and (b) pure MEK and p(MA/EGDMA) SLPs prepared at 5%C and 18%M in (c) 70:30%w/w MEK:heptane and (d) pure MEK.

polymerisation did not affect the mechanism of polymer formation. However, it was observed that the RI traces for the MEK/heptane polymerisation (Fig. 7c) were shifted into regions of higher retention volumes, indicating the formation of lower M_w SLPs and an increased formation of p(MA) homopolymers compared to the single solvent system.

The concentration effect caused by the addition of heptane to the MA/EGDMA polymerisation did not have the same effect as for the MMA/EGDMA polymerisation system as a result of the sterically hindered double bonds present on the cores of the p(MA/EGDMA) SLPs. The observed decrease in M_w with increasing heptane concentration for the p(MA/EGDMA) system results from the less extended conformation of the p(MA) 'arms' of the SLPs in the binary solvent as a result of the overall poorer solvating environment, compared to a pure MEK environment. This results in an increased shielding of the pendent double bonds present in the cores, hindering intermolecular cross-linking reactions, which leads to the formation of lower M_w SLPs. This phenomenon dominates over the concentration effect, observed for the p(MMA/EGDMA) system. This also leads to the increased homopolymerisation of MA dominating in the latter stages of the reaction, resulting in a decrease in the M_w by virtue of the production of low M_w p(MA) polymers.

The absence of a high M_w shoulder in the GPC RI traces (Fig. 7a and b) for the homopolymerisation of MA (which resemble the results obtained for the homopolymerisation of MMA (Fig. 4a and b)) demonstrates that the high M_w shoulder (Fig. 7c and d, Region 1) for the MA/EGDMA polymerisation is a result of the formation of SLPs. These results clearly indicate that the rapid consumption of EGDMA during the initial stages of the reaction is responsible for the formation of SLPs.

To further illustrate the structural differences between the p(MA/EGDMA) SLPs and branched p(MMA/EGDMA) polymers, the conformational plots of the products obtained after their respective kinetic studies are shown in Fig. 8. As mentioned previously, the theoretical values of α for spheres, random coils in theta solvents and rigid rods are 0.33, 0.60 and 1.0 [27], respectively. The α values of the respective products indicate that the p(MA/EGDMA) SLPs have a more spherical structure compared to the branched p(MMA/EGDMA) polymers. The presence of branching within these polymers is also supported by the lower α values of the p(MA/EGDMA) and p(MMA/EGDMA) polymers ($\alpha = 0.33$ and 0.41, respectively) compared with the p(MA) and p(MMA) homopolymers ($\alpha = 0.44$ and 0.54, respectively).
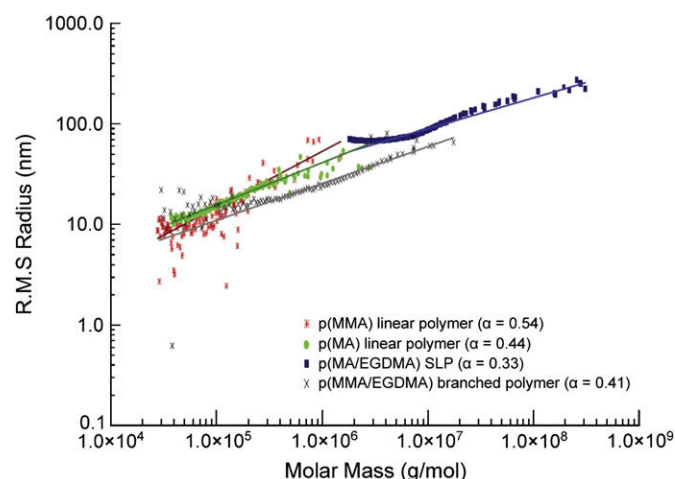

Fig. 8. Conformational plots of p(MMA) and p(MA) linear homopolymers, branched p(MMA/EGDMA) polymers and p(MA/EGDMA) SLPs.

The evolution of α with time was also plotted for the different polymer systems to elucidate the structural changes during the polymerisation process (Fig. 9). Regions of low retention volumes (Fig. 9a and b) were analysed to minimise the influence of linear polymers on the value of α. Interestingly, a relatively sudden increase in the α value was observed between 7 and 10 h for the branched p(MMA/EGDMA) polymers (from $\alpha = 0.32$ to 0.41) while it remained relatively constant for the p(MA/EGDMA) SLPs (ca. $\alpha = 0.33$). The change from $\alpha = 0.32$ to 0.41 for the branched p(MMA/EGDMA) polymers corresponded exactly with the complete consumption of EGDMA. This indicates that more compact structures were formed during the initial stages of polymerisation with the incorporation of EGDMA into the polymeric architecture. However, after the complete consumption of EGDMA, the accessibility of the pendent vinyl groups present on the polymers allowed further intermolecular reactions to occur, resulting in the formation of the expected branched polymers. In contrast, the α value of the p(MA/EGDMA) SLPs remained constant (ca. $\alpha = 0.33$) indicating that the rapid consumption of EGDMA during the initial stages of the reaction resulted in the formation of the SLPs with any pendent vinyl groups present in the cores of the SLPs sterically hindered from further reaction. As expected, the p(MA) and p(MMA) α values remain consistently larger than the p(MA/EGDMA) SLPs and branched p(MMA/EGDMA) polymers due to the lack of branching present within these homopolymers.

3.5. Incorporation of surfmers

It has previously been demonstrated that long-chained acrylate monomers incorporated into cross-linked microparticles synthesised via dispersion polymerisation, have the ability to stabilise these particles with the stability being dependent on the length of the surfmer [12]. In this study, octadecyl acrylate (ODA) was chosen as the surfmer to determine if the combined effect of monomer reactivity control and surfmer incorporation would affect the gelation limits of the MA/EGDMA and MMA/EGDMA polymerisation systems.

3.6. Effectiveness of ODA as a surfmer

Initially, experiments were conducted to determine the minimum concentration of ODA that would be required to delay macrogelation of the p(MMA/EGDMA) system. By substitution of the mono-vinyl monomer with 1, 5 and 10%w/w of ODA, it was determined that a minimum concentration of 10%w/w of ODA was required (Table 5) at a formulation of 3%C and 23%M. It was also demonstrated that the use of surfmers without incorporating the binary solvent system was not effective in delaying the onset of macrogelation.

Domain diagrams for the p(MMA/ODA/EGDMA) and p(MA/ODA/EGDMA) systems were experimentally determined using 90:10%w/w MMA or MA:ODA, and 80:20 and 70:30 MEK:heptane solvent mixtures (Figs. 10 and 11, respectively).

Fig. 10 indicates that the gelation boundary for the p(MMA/EGDMA) system has been further extended by ca. 3%M when ODA was employed as the surfmer, which equates to an increase in polymer yield of 11–17 ± 4%w/w across the gelation boundary [26]. This can be accounted for by considering the effect of monomer reactivity ratios on the polymer composition. For example, the reactivity ratios between $M_1 = $ MMA and $M_2 = $ ODA are $r_1 = 2.36 \pm 0.04$ and $r_2 = 0.48 \pm 0.12$ [33], indicating that ODA has a higher propensity to cross-propagate. Given that the reactivity of methacrylates is higher than acrylates, branched polymers with peripheral ODA groups would be formed. These ODA groups act as surfmers, stabilising the polymers and shielding them from further intermolecular reaction [13]. The reduced M_w and hydrodynamic
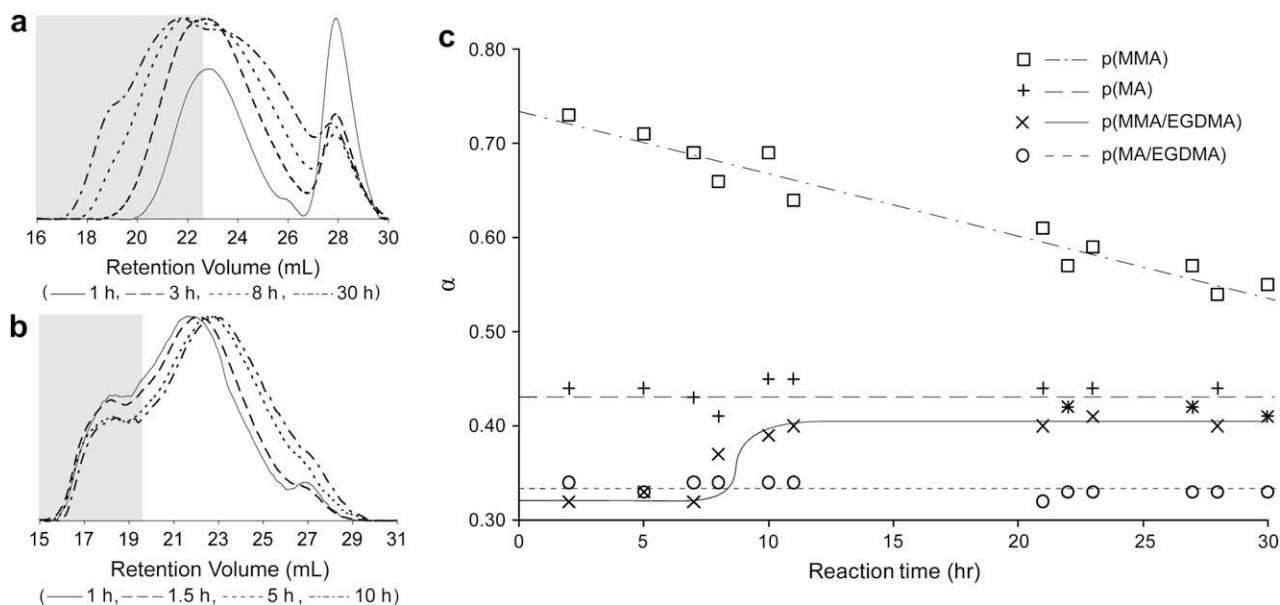
Fig. 9. Kinetic evolution of α with reaction time. Shaded regions of (a) p(MMA/EGDMA) and (b) p(MA/EGDMA) kinetic traces indicate the areas analysed.

Table 5
Results from MMA/ODA/EGDMA polymerisations with increasing ODA content at a formulation of 3%C and 23%M.

Polymer	ODA content %w/w[a]	Solvent composition %w/w heptane	M_w[b] (kDa)	PDI[b]	Yield[d] (%)
P3a	1	0	–[c]	–	–
P3b	5	0	–[c]	–	–
P3c	10	0	–[c]	–	–
P3d	1	20	–[c]	–	–
P3e	5	20	–[c]	–	–
P3f	10	20	2990	3.5	70.5
P3g	1	30	–[c]	–	–
P3h	5	30	–[c]	–	–
P3i	10	30	2520	3.8	74.0

[a] Represents the weight percentage of mono-vinyl monomer replaced by ODA.
[b] Determined by GPC–MALLS.
[c] Insoluble gel formation.
[d] Determined gravimetrically.

diameter (d_h) of the p(MMA/ODA/EGDMA) compared to the p(MMA/EGDMA) polymers synthesised at identical formulations (Table 6 and Fig. 12) support the hypothesis that the incorporated surfmers stabilise the polymers by sterically shielding the vinyl bonds located within them from further cross-linking reactions. Therefore, resulting in the formation of lower M_w branched polymers.

In comparison, attempts to extend the gelation limits in the p(MA/ODA/EGDMA) systems were unsuccessful (Fig. 11). This is attributed to the burial of the surfmers within the SLP structure [10,11,34,35] as a result of the similar reactivity of MA and ODA on account of them both being acrylates. Given that the reactivity ratios between MMA/MA and MMA/ODA are similar, then we would expect the reactivity difference between ODA and MA to be minimal. This would lead to the formation of SLPs with most of the ODA groups buried within the polymer preventing them from sterically shielding the polymers from further reaction.
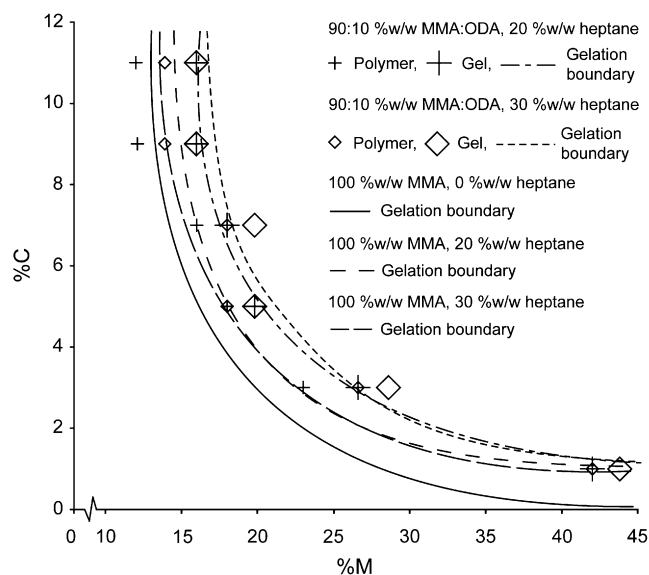

Fig. 10. Domain diagram for p(MMA/ODA/EGDMA) system synthesised by CFRP in MEK:heptane 80:20 and 70:30%w/w at 70 °C for 20 h, using AIBN as the initiator.
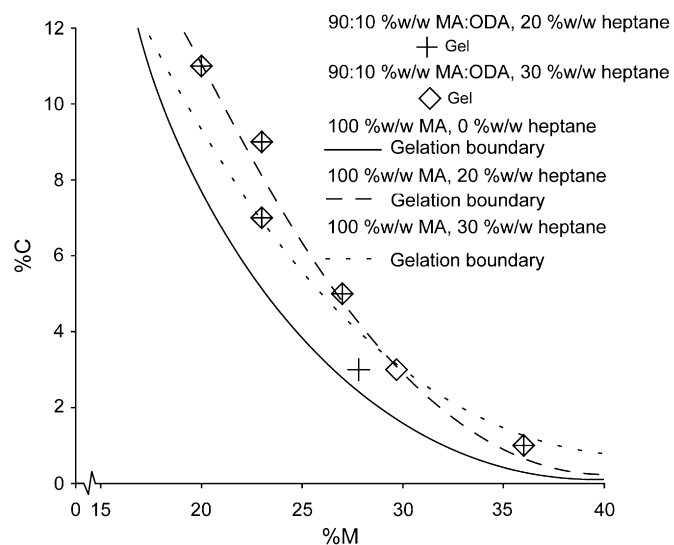

Fig. 11. Domain diagram for p(MA/ODA/EGDMA) system synthesised by CFRP in MEK:heptane 80:20 and 70:30%w/w at 70 °C for 20 h, using AIBN as the initiator.

Table 6
M_w and d_h comparisons between branched p(MMA/ODA/EGDMA) and p(MMA/EGDMA) polymers synthesised in 70:30%w/w MEK:heptane at various formulations.

Polymer	Formulation		Mono-vinyl monomer %w/w MMA:ODA	M_w[a] (kDa)	PDI[a]	d_h[b] (nm)	Yield[c] (%)
	%C	%M					
P1b	3	20	100:0	5600	3.7	58.9	70.8
P4a	3	20	90:10	2340	2.6	24.5	67.9
P1d	5	16	100:0	5530	4.6	62.4	73.7
P4b	5	16	90:10	1710	5.3	10.7	71.6
P1f	7	12	100:0	814	11.8	6.1	74.0
P4c	7	12	90:10	395	4.0	4.6	70.5

[a] Determined by GPC–MALLS.
[b] Determined by DLS.
[c] Determined gravimetrically.

Table 7
Properties of fractionated p(MMA/ODA/EGDMA) and p(MA/ODA/EGDMA) polymers.

Polymer	Mono-vinyl monomer	Formulation		Solvent composition %w/w heptane	M_w[a] (kDa)	PDI[a]
		%C	%M			
P3j	MMA	5	18	20	4940	2.0
P3j[φ]	MMA	5	18	20	14,300	1.2
P3k	MA	1	34	20	490	6.3
P3k[φ]	MA	1	34	20	2730	1.1

The superscript φ denotes the fractionated samples.
[a] Determined by GPC–MALLS.

3.7. Confirmation of surfmer incorporation

Given the potential for compositional drift to occur in these systems, it is important to confirm that the surfmers have been incorporated into the branched polymers. To determine this, ^{13}C NMR spectroscopic analysis was conducted on fractionated samples (Table 7) of p(MMA/EGDMA) and p(MA/EGDMA) polymers, and their ODA analogues (Figs. 13 and 14, respectively). Fractionation of the samples was conducted to remove the presence of the low M_w linear and branched polymers formed during the polymerisation and allow the analysis of the high M_w polymeric species in both polymerisation systems to determine if ODA has been successfully incorporated into the branched and star-like polymer architectures.

Resonances observed at $\delta_c = 29.7$ ppm (Figs. 13a and 14a) are characteristic of long alkyl chain methylene group carbons and confirm the incorporation of ODA into the branched polymers. This confirms that the inability in extending the macrogelation limit in
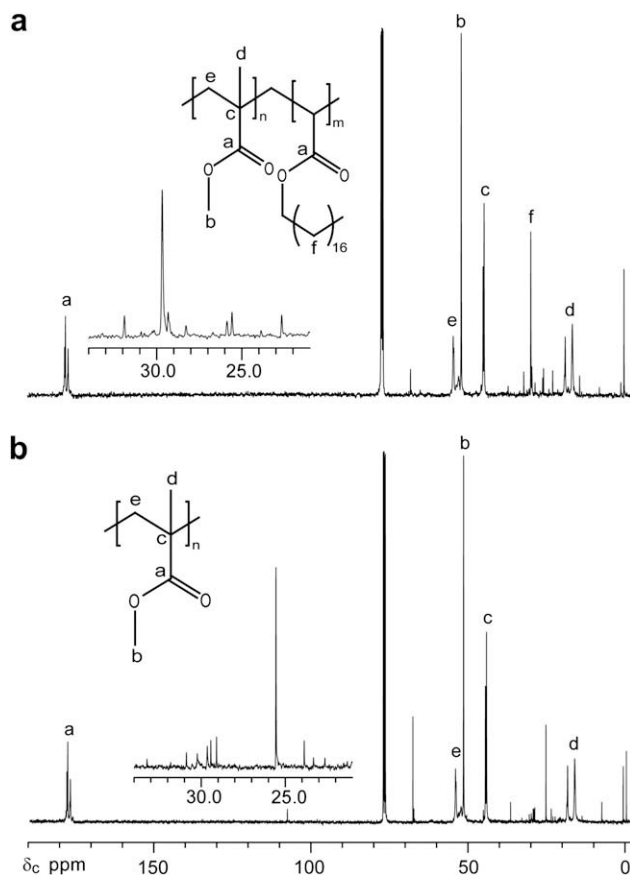

Fig. 12. DLS analysis of branched p(MMA/EGDMA) and p(MMA/ODA/EGDMA) polymers.

Fig. 13. ^{13}C NMR spectra (100 MHz, CDCl₃) of fractionated; (a) p(MMA/ODA/EGDMA) P3j[φ] and (b) branched p(MMA/EGDMA) P3j polymers.
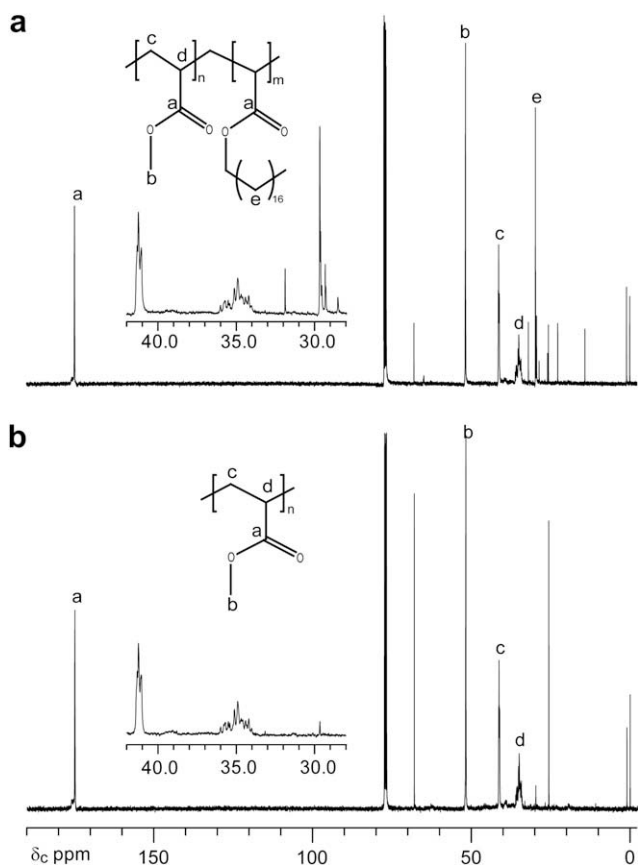
Fig. 14. ^{13}C NMR spectra (100 MHz, CDCl$_3$) of fractionated (a) p(MA/ODA/EGDMA) P3k$^\phi$ and (b) p(MA/EGDMA) P3k SLPs.

the p(MA/ODA/EGDMA) system results from surfmer burial and not non-incorporation of ODA into the polymeric structure as a result of compositional drift.

3.8. Effectiveness of vinyl stearate as a surfmer

With the unsuccessful delay in gelation of the p(MA/ODA/EGDMA) attributed to surfmer burial, vinyl stearate (VS), which has a much lower reactivity than MA, was subsequently used as a surfmer to determine if gelation could be delayed. For the copolymerisation of MA and VS, the reactivity ratios between
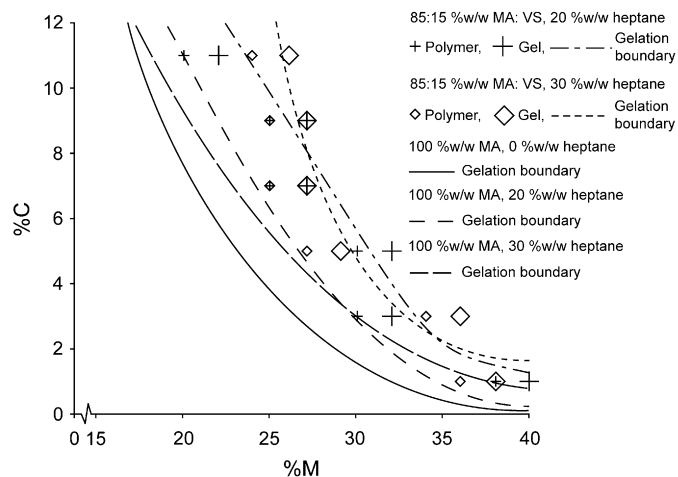

Fig. 15. Domain diagram for p(MA/VS/EGDMA) system synthesised by CFRP in MEK:heptane 80:20 and 70:30%w/w at 70 °C for 20 h, using AIBN as the initiator.

Table 8
M_ws of p(MA/VS/EGDMA) polymers using 85:15%w/w MA/VS synthesised at various formulations.

Polymer	Formulation		Solvent composition %w/w heptane	M_w[a] (kDa)	PDI[a]	Yield[b] (%)
	%C	%M				
P5a	1	36	20	511	4.9	59.0
P5b	3	30	20	1050	3.4	56.3
P5c	7	25	20	2510	3.8	50.4
P5d	9	25	20	3720	2.6	48.5
P5e	11	20	20	1440	3.9	63.7
P6a	1	36	30	526	4.3	55.3
P6b	3	30	30	669	2.4	55.1
P6c	7	25	30	1200	2.5	54.5
P6d	9	25	30	1080	2.6	43.5
P6e	11	20	30	1410	2.5	59.0

[a] Determined by GPC–MALLS.
[b] Determined gravimetrically.

M$_1$ = MA and M$_2$ = VS were reported to be $r_1 = 5.8$ and $r_2 = 0.03$ [17]. The domain diagram for the p(MA/VS/EGDMA) system was determined using 85:15%w/w MA/VS in 80:20 and 70:30 MEK:heptane solvent mixtures (Fig. 15).

Fig. 15 indicates a further increase of *ca.* 4%*M* for the gelation limit of the p(MA/EGDMA) polymer system with the incorporation of VS into the SLPs, which equates to an increase in polymer yield of 8–20 ± 5%w/w across the gelation boundary [26]. The properties of the p(MA/VS/EGDMA) polymers are listed in Table 8. This supports the hypothesis that surfmers located at the periphery of the SLPs are effective in shielding them from further reaction. The decreasing M_w trend of the polymers synthesised with increasing heptane concentration is also observed for the p(MA/VS/EGDMA) system. As before, ^{13}C NMR spectroscopic analysis of the p(MA/VS/EGDMA) SLPs reveals resonances corresponding to alkyl methylene carbons of VS, confirming its incorporation into the SLP architecture.

4. Conclusions

Branched p(MMA/EGDMA) and star-like p(MA/EGDMA) polymers were synthesised *via* CFRP and their gelation limits were successfully extended by exploiting the polymer conformational changes in a binary solvent mixture. Contrasting M_w trends observed for the two systems were explained by comparing the effect of the reactivity of the different monomers used in both systems and the addition of heptane into the reaction mixtures. Conformational plots were used to illustrate the architectural differences between the different polymers which further support the observed M_w trends. It was demonstrated that the concentration effect caused by the addition of heptane led to an increase in the M_w of the branched p(MMA/EGDMA) polymers. This was attributed to the increased accessibility of the unreacted pendent double bonds to intermolecular cross-linking and the increased proximity of the polymers as a result of their residence in a constrained good solvent environment. The decreasing M_w trend of the more compact p(MA/EGDMA) polymers resulted from the collapsed structure of the p(MA/EGDMA) SLPs in a poor solvent environment shielding the vinyl bonds present within the core. The increased proximity of these polymers within the good solvent environment in this case does not play a dominant role in affecting the M_w of the SLPs due to the sterically hindered vinyl bonds. This lowered the M_w of the synthesised SLPs and led to an increased formation of low M_w linear p(MA) homopolymers. This demonstrates the potential for concentrating batch reaction mixtures without resulting in macrogelation by the addition of small amounts of precipitant into the reaction solution.

When surfmers were incorporated into the polymers, it was found that the positioning of these groups within the polymer architecture played a crucial part in determining their ability to delay macrogelation. It has been shown that surfmer chains located at the periphery of the polymers, as in the case of the branched p(MMA/ODA/EGDMA) and star-like p(MA/VS/EGDMA) polymers delayed the onset of macrogelation by sterically shielding the unreacted double bonds from further intermolecular reaction, while p(MA/ODA/EGDMA) SLPs, which had the surfmers buried within the polymer, could not effectively delay macrogelation.

It was demonstrated that total increases in p(MMA/EGDMA) and p(MA/EGDMA) polymers yields of $14–57 \pm 6\%$w/w and $25–35 \pm 5\%$w/w, respectively, were achieved employing a combination of the binary solvent and surfmer systems. The methods detailed here have the potential to increase the commercial viability and reduce the environmental impact of the synthesis of these branched and SLPs *via* the one-pot CFRP process by reducing the amount of solvent required for the production process. This process would also have the potential of allowing the facile synthesis of highly branched polymer products by reducing their tendency to gel by the simple addition of small amounts of precipitant and a low reactivity surfmer into the reaction mixture.

Acknowledgements

References

[1] Tsitsilianis C, Graff S, Rempp P. Eur Polym J 1991;27:243.
[2] Worsfold DJ, Zilliox JG, Rempp P. Can J Chem 1969;47:3379.
[3] (a) Abrol S, Caulfield MJ, Qiao GG, Solomon DH. Polymer 2001;42:5987;
(b) Abrol S, Kambouris PA, Looney MG, Solomon DH. Macromol Rapid Commun 1997;18:755;
(c) Bosman AW, Vestberg R, Heumann A, Fréchet JMJ, Hawker CJ. J Am Chem Soc 2003;125:715;
(d) Solomon DH, Abrol S, Kambouris PA, Looney MG. A process for preparing polymeric microgels. WO 9,831,739; 1998.
[4] (a) Baek KY, Kamigaito M, Sawamoto M. Macromolecules 2001;34:7629;
(b) Baek KY, Kamigaito M, Sawamoto M. Macromolecules 2001;34:215;
(c) Baek KY, Kamigaito M, Sawamoto M. J Polym Sci A Polym Chem 2002;40:1972;
(d) Baek KY, Kamigaito M, Sawamoto M. J Polym Sci A Polym Chem 2002;40:633;
(e) Baek KY, Kamigaito M, Sawamoto M. Macromolecules 2002;35:1493;
(f) Gurr PA, Qiao GG, Solomon DH, Harton SE, Spontak RJ. Macromolecules 2003;36:5650;
(g) Solomon DH, Qiao GG, Abrol S. Process for microgel preparation. WO 9,958,588; 1999.
(h) Xia J, Zhang X, Matyjaszewski K. Macromolecules 1999;32:4482;
(i) Zhang X, Xia J, Matyjaszewski K. Macromolecules 2000;33:2340.
[5] Connal LA, Gurr PA, Qiao GG, Solomon DH. J Mater Chem 2005;15:1286.
[6] (a) Lord HT, Quinn JF, Angus SD, Whittaker MR, Stenzel MH, Davis TP. J Mater Chem 2003;13:2819;
(b) Moad G, Mayadunne RTA, Rizzardo E, Skidmore M, Thang SH. Macromol Symp 2003;192:1;
(c) Zheng G, Pan C. Polymer 2005;46:2802.
[7] Ho AK, Iin I, Gurr PA, Mills MF, Qiao GG. Polymer 2005;46:6727.
[8] Peppas NA, Nagai T, Miyajima M. Pharm Technol Jpn 1994;10:611.
[9] (a) Aramendia E, Barandiaran MJ, Asua JM. C R Chim 2003;6:1313;
(b) Matahwa H, McLeary JB, Sanderson RD. J Polym Sci A Polym Chem 2005;44:427.
[10] Aramendia E, Barandiaran MJ, Grade J, Blease T, Asua JM. J Polym Sci A Polym Chem 2002;40:1552.
[11] Unzue MJ, Schoonbrood HAS, Asua JM, Goni AM, Sherrington DC, Stahler K, et al. J Appl Polym Sci 1997;66:1803.
[12] Valette L, Pascault JP, Magny B. Macromol Mater Eng 2002;287:31.
[13] (a) Bentley J, Lambourne R, Strivens TA, editors. Paint and surface coatings. 2nd ed. Cambridge, UK: Woodhead Publishing; 1999;
(b) Kawaguchi S, Ito K. Adv Polym Sci 2005;175:299;
(c) Klein SM, Manoharan VN, Pine DJ, Lange FF. Colloid Polym Sci 2003;282:7.
[14] Wang W, Zheng Y, Roberts E, Duxbury CJ, Ding L, Irvine DJ, et al. Macromolecules 2007;40:7184.
[15] For this article, the term 'binary solvent' will denote a homogeneous solvent mixture comprising of a precipitant for the polymer and a good solvent for the polymer.
[16] Kwok AY, Neo SA, Qiao GG, Solomon DH. J Appl Polym Sci 2005;98:1462.
[17] Brandrup J, Immergut EH, Grulke EA, editors. Polymer handbook. 4th ed. Chichester, UK: Wiley-Interscience; 1998.
[18] Boots HMJ, Kloosterboer JG, Serbutoviez C, Touwslager FJ. Macromolecules 1996;29:7683.
[19] Cameron GG, Cameron J. Polymer 1973;14:107.
[20] Cowie JMG. J Polym Sci Polym Symp 1968;23:267.
[21] (a) Berek D, Bleha T, Pevna Z. J Polym Sci Polym Lett Ed 1976;14:323;
(b) Huyskens PL, Haulait-Pirson MC, Vandevyvere P, Seghers K, Zeegers-Huyskens T. J Chem Soc Faraday Trans 1998;94:3587;
(c) Katime IA, Ochoa JR, Teijon JM. J Chem Soc Faraday Trans 2 1985;81:783;
(d) Kwok AY, Qiao GG, Solomon DH. Polymer 2003;44:6195;
(e) Venkatesu P. J Chem Phys 2005;123:024902/1;
(f) Venkatesu P. J Phys Chem B 2006;110:17339;
(g) Gromov VF, Bogachev YS, Bune EV, Zhuravleva IL, Teleshov EN. Eur Polym J 1991;27:505.
[22] Horta A, Katime IA. Macromolecules 1984;17:2734.
[23] Archer AJ, Evans R. J Chem Phys 2003;118:9726.
[24] The term 'environment' is used to denote a transient phenomenon rather than distinctly separated 'phases' such as observed in heterogeneous polymerisations.
[25] Wypych G, editor. Handbook of solvents. Toronto, Ontario: ChemTec Publishing; 2001.
[26] Determined via conversion data and gravimetric analyses.
[27] (a) Andersson M, Wittgren B, Wahlund KG. Anal Chem 2003;75:4279;
(b) Podzimek S, Vlcek T. J Appl Polym Sci 2001;82:454.
[28] Balke ST, Hamielec AE. J Appl Polym Sci 1973;17:905.
[29] Huang HM, Liu IC, Tsiang RCC. Polymer 2005;46:955.
[30] Daoud M, Cotton JP. J. Phys 1982;43:531.
[31] (a) Buback M, Mueller E. Macromol Chem Phys 2007;208:581;
(b) Semsarzadeh MA, Daronkola MRR, Abdollahi M. J Macromol Sci Pure Appl Chem 2007;44:953.
[32] Matyjaszewski K, Ziegler MJ, Arehart SV, Greszta D, Pakula T. J Phys Org Chem 2000;13:775.
[33] Bamford CH, Tipper CFH, editors. Comprehensive chemical kinetics: free radical polymerization, vol. 14A. New York: Elsevier; 1976.
[34] Sindt O, Gauthier C, Hamaide T, Guyot A. J Appl Polym Sci 2000;77:2768.
[35] Schoonbrood HAS, Unzue MJ, Beck OJ, Asua JM, Goni AM, Sherrington DC. Macromolecules 1997;30:6024.